Stem Cell Reports
Article
ISSCR
OPEN ACCESS

The histone acetyltransferase KAT6B is required for hematopoietic stem cell development and function

Maria I. Bergamasco,[1,2] Nishika Ranathunga,[1,2] Waruni Abeysekera,[1,2] Connie S N Li-Wai-Suen,[1,2] Alexandra L. Garnham,[1,2] Simon N. Willis,[1,2] Helen M. McRae,[1,2] Yuqing Yang,[1,2] Angela D'Amico,[1,2] Ladina Di Rago,[1,2] Stephen Wilcox,[1,2] Stephen L. Nutt,[1,2] Warren S. Alexander,[1,2] Gordon K. Smyth,[1,3] Anne K. Voss,[1,2,4,*] and Tim Thomas[1,2,4,5,*]

[1]The Walter and Eliza Hall Institute of Medical Research, Melbourne, VIC 3052, Australia
[2]Department of Medical Biology, University of Melbourne, Melbourne, VIC 3052, Australia
[3]Department of Mathematics and Statistics, University of Melbourne, Melbourne, VIC 3010, Australia
[4]These authors contributed equally
[5]Lead contact
*Correspondence: tthomas@wehi.edu.au (A.K.V.), avoss@wehi.edu.au (T.T.)
https://doi.org/10.1016/j.stemcr.2024.02.005

SUMMARY

The histone lysine acetyltransferase KAT6B (MYST4, MORF, QKF) is the target of recurrent chromosomal translocations causing hematological malignancies with poor prognosis. Using *Kat6b* germline deletion and overexpression in mice, we determined the role of KAT6B in the hematopoietic system. We found that KAT6B sustained the fetal hematopoietic stem cell pool but did not affect viability or differentiation. KAT6B was essential for normal levels of histone H3 lysine 9 (H3K9) acetylation but not for a previously proposed target, H3K23. Compound heterozygosity of *Kat6b* and the closely related gene, *Kat6a,* abolished hematopoietic reconstitution after transplantation. KAT6B and KAT6A cooperatively promoted transcription of genes regulating hematopoiesis, including the *Hoxa* cluster, *Pbx1*, *Meis1, Gata* family, *Erg,* and *Flt3*. In conclusion, we identified the hematopoietic processes requiring *Kat6b* and showed that KAT6B and KAT6A synergistically promoted HSC development, function, and transcription. Our findings are pertinent to current clinical trials testing KAT6A/B inhibitors as cancer therapeutics.

INTRODUCTION

The MYST (MOZ, Ybf2/Sas3, Sas2, TIP60) family histone lysine acetyltransferase KAT6B is the target of recurrent chromosomal translocations causing hematological abnormalities with weak responses to chemotherapy and poor patient outcomes (Panagopoulos et al., 2001; Vizmanos et al., 2003). KAT6B fusion to the CREB binding protein (CBP) results in acute myeloid leukemia (AML) and myelodysplastic syndrome (Panagopoulos et al., 2001; Vizmanos et al., 2003). Interestingly, enhancers associated with KAT6B show prominent age-related epigenetic reprogramming in hematopoietic stem cells (HSCs) (Adelman et al., 2019). The risk of hematological malignancy increases with age and epigenetic changes to human HSCs have been suggested to create a predisposition for the development of age-related leukemia (Adelman et al., 2019).

In addition to hematological malignancy, *de novo* mutations in the human *KAT6B* gene lead to distinct congenital disorders defined by intellectual disability and skeletal abnormalities (Campeau et al., 2012; Kraft et al., 2011; Simpson et al., 2012). Say-Barber-Biesecker-Young-Simpson (SBBYS) syndrome is characterized by intellectual disability; an immobile, mask-like face; blepharophimosis; ptosis; and long first digits (Clayton-Smith et al., 2011). In contrast, mutations in a discreet region of the *KAT6B* gene that cause Genitopatellar syndrome, characterized by a global developmental delay, underdeveloped or absent patellae, and urogenital abnormalities (Simpson et al., 2012), have been proposed to confer an abnormal gain of function (Campeau et al., 2012). As most patients receive a genetic diagnosis early in life, whether malignancies arise in later life remains to be determined.

KAT6B shares identical domain structure and high sequence similarity with another MYST family member, KAT6A (MYST3, MOZ, monocytic leukemia zinc finger) (Champagne et al., 1999; Thomas et al., 2000). KAT6A is similarly the target of recurrent chromosomal translocations leading to AML with poor patient responses to chemotherapy and short median survival (Borrow et al., 1996). Endogenous KAT6A is essential for normal hematopoiesis. Loss of function of KAT6A results in an absence of fetal HSCs, failure to reconstitute an irradiated transplant recipient (Katsumoto et al., 2006; Thomas et al., 2006), and failure to maintain phenotypic HSCs in adulthood (Sheikh et al., 2016). Furthermore, KAT6A is required to maintain the quiescent, non-cycling HSC pool (Sheikh et al., 2017), which is thought to be critical for the lifespan of HSCs. Since recently developed small molecule inhibitors targeting both KAT6A and KAT6B have been shown to arrest lymphoma (Baell et al., 2018) and breast cancer growth (Sharma et al., 2023) in animal models and are already in clinical trials for the treatment of cancer, it is essential for the well-being of people receiving the

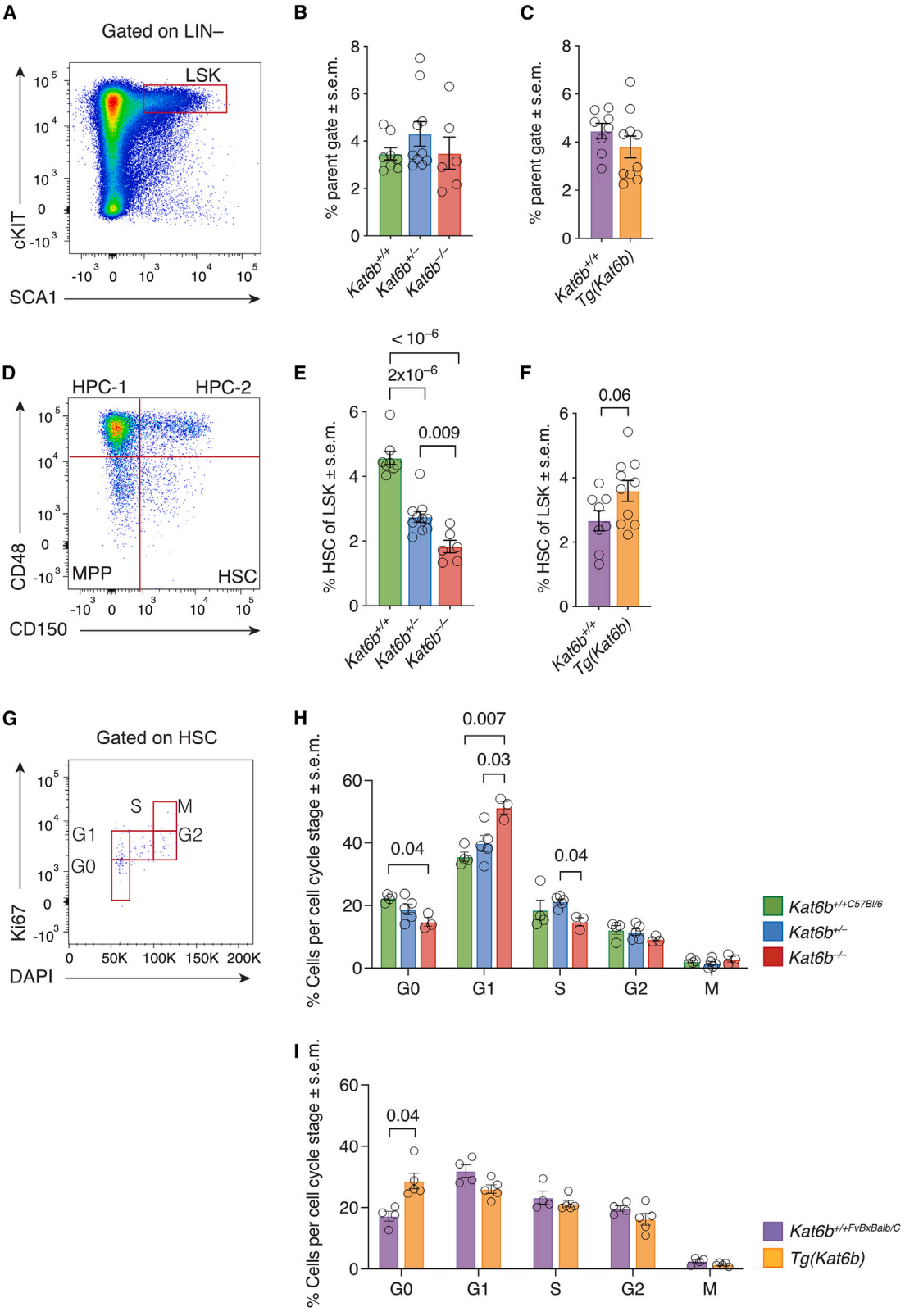

(legend on next page)

treatment to establish the effects of KAT6B on hematopoietic cell proliferation, survival, and function.

To resolve this question, we examined the effects of gain and loss of function of KAT6B and the interaction of KAT6B with KAT6A in the hematopoietic system.

RESULTS

Kat6b gene deletion results in a reduction in the percentage of fetal liver HSCs

Exons 2–12 of the *Kat6b* gene were deleted to produce a null allele, *Kat6b*$^{-}$, that removed all transcripts resulting from alternative splicing and alternative promoter use (Thomas et al., 2000) at the *Kat6b* locus (Figure S1).

Kat6b overexpressing transgenic mice (*Tg(Kat6b)*) had seven additional copies of *Kat6b* and a 5-fold increase in *Kat6b* expression (Figure S1). *Kat6b*$^{-/-}$ and *Tg(Kat6b)* animals were indistinguishable from littermate controls at E14.5 (Figure S1). *Kat6b*$^{-/-}$ died perinatally. *Tg(Kat6b)* heterozygous mice were viable only on a mixed genetic background (FVB:BALB/c). *Kat6b*$^{+/-}$, *Kat6b*$^{-/-}$, and *Tg(Kat6b)* animals and their respective wild-type controls were genotyped using primers in Table S1.

Hematopoietic stem and progenitor cell populations were assessed in the E14.5 fetal liver by flow cytometry using antibodies to cell surface markers (Tables S2 and S3). No differences were observed in the numbers of LIN^{-}SCA1^{+}KIT^{+} stem and progenitor cells (LSK cells) in either mutant relative to their control (Figures 1A–1C). In contrast, the percentage of CD48^{-}CD150^{+} hematopoietic stem cells (HSCs) within fetal liver LSK cells was reduced after loss of one or two alleles of *Kat6b* in a gene-dose dependent manner by 40% ($p = 2 \times 10^{-6}$) and 60% ($p < 10^{-6}$), respectively (Figures 1D and 1E). *Tg(Kat6b)* E14.5 fetal livers trended toward an increase in HSCs, although this did not reach statistical significance (p = 0.06; Figure 1F).

To determine if the *Tg(Kat6b)* transgene insertion encoded functional KAT6B protein, *Tg(Kat6b)* mice were crossed to *Kat6b*$^{+/-}$ animals. The offspring were backcrossed to FVB:BALB/c 4 generations (Figure S1). The decreased percentage of HSCs in *Kat6b*$^{-/-}$ E14.5 fetal liver LSK cells was restored to wild-type levels in *Kat6b*$^{-/-}$ samples that were also positive for the *Tg(Kat6b)* transgene (Figure S1).

Loss and gain of KAT6B affect HSC quiescence but not viability

Cell cycle and cell death were assessed in E14.5 fetal liver HSCs by Ki67/DAPI and annexin V/propidium iodine staining and flow cytometry, respectively. Loss of KAT6B resulted in a 44% reduction of HSCs in G0 (p = 0.04, Figures 1G and 1H) and a 44% increase in G1 phase of the cell cycle relative to controls (p = 0.007; Figures 1G and 1H). Conversely, more *Tg(Kat6b)* HSCs were found in G0 (167%, p = 0.04; Figure 1I). No difference was observed in HSC viability across *Kat6b* genotypes (Figure S1).

Loss or gain of KAT6B affects colony numbers but does not affect HSC differentiation *in vitro*

To determine the effect of KAT6B on HSC differentiation, *in vitro* colony-forming assays (Metcalf, 1984) were performed. *Kat6b*$^{-/-}$ fetal liver cells formed 70% fewer colonies (p = 0.008; Figure 2A), with colony sizes 24% smaller, on average (p = 0.04; Figure 2B). No difference in colony type proportions was observed across genotypes (Figure 2C). However, 40% more colonies arose from *Tg(Kat6b)* cells (p = 0.002; Figure 2D); these were of a comparable size to those arising from control cells (Figure 2E). KAT6B gain did not affect colony type proportion (Figure 2F), indicating that loss or gain of KAT6B function did not affect HSC differentiation *in vitro*.

Loss of KAT6B impairs hematopoietic reconstitution of irradiated recipients

The requirement for KAT6B in HSC function was assessed by competitive transplantation experiments; 5×10^5 fetal liver test cells (CD45.2^{+}) from *Kat6b*$^{-/-}$, *Kat6b*$^{+/-}$, or wild-type E14.5 fetuses were combined with 1×10^6 adult bone marrow competitor cells (CD45.1^{+}) and injected

Figure 1. Deletion of *Kat6b* alleles results in a gene-dose-dependent reduction in the percentage of E14.5 fetal liver hematopoietic stem cells

(A) Representative flow cytometry plot of LSK cells in the E14.5 fetal liver.

(B and C) LSK cell percentage in *Kat6b*$^{+/+C57BL/6}$, *Kat6b*$^{+/-}$ and *Kat6b*$^{-/-}$ (B), or *Kat6b*$^{+/+FVBxBALB/c}$ and *Tg(Kat6b)* (C) overexpressing E14.5 fetal livers.

(D) Representative flow cytometry plot.

(E and F) Percentage of HSCs in *Kat6b*$^{+/-}$ and *Kat6b*$^{-/-}$ mice compared with controls (E) and *Tg(Kat6b)* mice compared with controls (F).

(G) Representative flow cytometry plot of Ki67 vs. DAPI in HSCs.

(H and I) Cell cycle quantitation for HSCs from *Kat6b*$^{+/-}$ and *Kat6b*$^{-/-}$ mice compared with controls (H) and *Tg(Kat6b)* mice compared with controls (I). n = 6–10 (A), 8–10 (B), 6–10 (E), 8–10 (F), 3–5 (H), and 4–5 (I) mice per genotype. Data are presented as mean ± standard error of the mean (SEM). Each circle represents an individual mouse. Data were analyzed by one-way ANOVA with Tukey post hoc correction (B, E), Student's t test (C, F) or two-way ANOVA with Tukey (H) or Sidak post hoc correction (I).

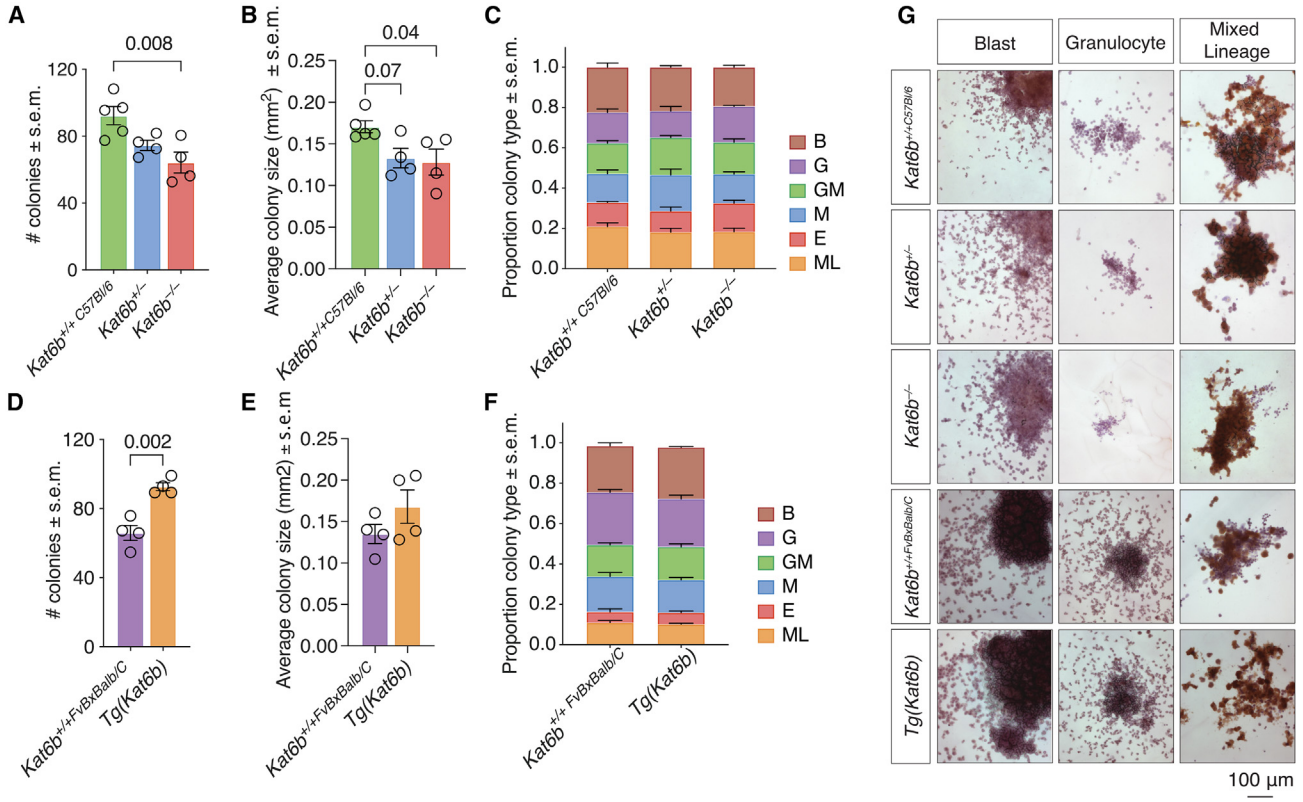

Figure 2. Loss and gain of *Kat6b* reduces and enhances hematopoietic progenitor colony formation, respectively, but neither affects differentiation *in vitro*

(A and B) Number (A) and average size (B) of colonies formed *in vitro* from *Kat6b*$^{+/+C57BL/6}$, *Kat6b*$^{+/-}$, and *Kat6b*$^{-/-}$ animals.

(C) Proportion colony types formed from *Kat6b*$^{+/+C57BL/6}$, *Kat6b*$^{+/-}$, and *Kat6b*$^{-/-}$ mice.

(D and E) Number (D) and average size (E) of colonies formed *in vitro* from *Kat6b*$^{+/+FVBxBALB/c}$ and *Tg(Kat6b)*animals.

(F) Proportion colony types formed from *Kat6b*$^{+/+FVBxBALB/c}$ and *Tg(Kat6b)* mice.

(G) Representative images of colonies. Scale bar, 100 µm. N = 4–5 mice per genotype. Data are presented as mean ± SEM, analyzed by one-way ANOVA (A and B), unpaired Student's t test (D and E) or two-way ANOVA with Tukey (C) or Sidak (F) post hoc correction. Data in (B) and (E) based on area assessments of 50 colonies per sample, per genotype. B: blast colony; G: granulocyte colony; GM: granulocyte/macrophage colony; M: megakaryocyte colony; E: erythroid colony; ML: mixed lineage colony.

intravenously (i.v.) into three CD45.1^{+} lethally irradiated recipient mice per donor (all C57BL/6; Figure 3A). Also, 5 × 10^{5} fetal liver cells (CD45.2^{+}) from *Tg(Kat6b)* or control E14.5 fetuses were combined with 1 × 10^{6} adult bone marrow competitor cells (CD45.1/2^{+}; F1 FVB:BALB/c hybrids) and injected into three CD45.1/2^{+} lethally irradiated recipients per donor (Figure S2).

Reconstitution was assessed in the peripheral blood at 4 weeks (revealing short-term progenitor capacity) and 20 weeks after transplantation (revealing stem cell capacity; Figures 3B–3D). At both timepoints, recipients of *Kat6b*$^{-/-}$ cells showed a reduction in the percentage of CD45.2^{+} cells across all cell types, relative to *Kat6b*$^{+/+}$ cell recipients (p = 0.05 to 0.0007). At 20 weeks post-transplantation, the contribution of *Kat6b*$^{-/-}$ cells to peripheral white blood cells was reduced by 64% compared with wild-type donor cells (p = 0.01), with one donor failing to reconstitute the recipient. At 20 weeks post-transplantation (Figure 3E), *Kat6b*$^{-/-}$ donor cell recipients had a 33%–75% reduction in CD45.2^{+} cells relative to *Kat6b*$^{+/+}$ cell recipients across all stem and progenitor cell types, which included HSCs, multipotent progenitors (MPPs), restricted hematopoietic progenitors type 1 and 2 (HPC-1, HPC-2), common myeloid progenitors (CMPs), granulocyte-macrophage progenitors (GMPs), megakaryocyte-erythrocyte progenitors (MEPs), and common lymphoid progenitors (CLPs) (p = 0.03 to 3 × 10^{-6}; Figures 3F and 3G).

No difference was observed in *Tg(Kat6b)* cell recipients relative to controls in peripheral blood cell population at 4 weeks or 20 weeks post-transplant (Figure S2). However, a 63%–126% increase in CD45.2^{+} cells was observed in *Tg(Kat6b)* cell recipients vs. wild-type controls in CMP,

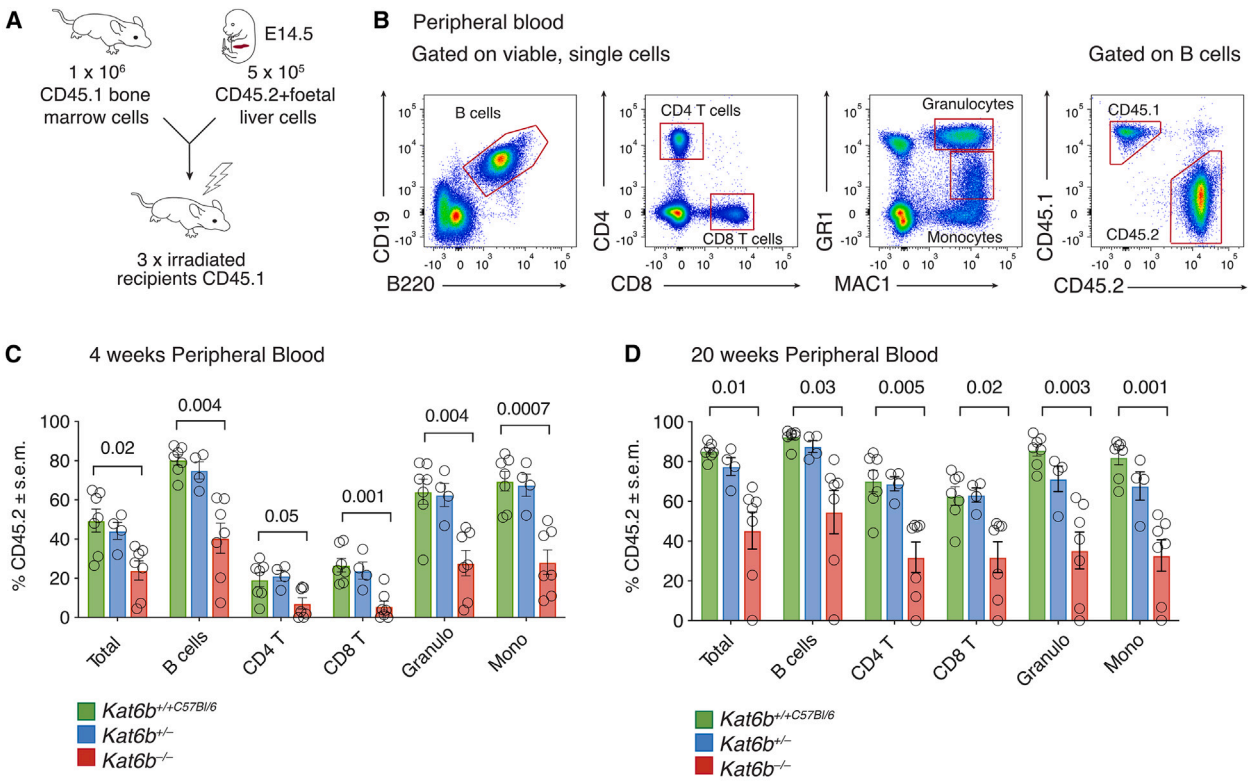

(legend on next page)

GMP, and MEP populations (lineage-specific progenitors), but not in stem cell populations (p = 0.02 to 0.002; Figure S2).

Short-term *in vivo* homing transplantation experiments demonstrated no difference in the engraftment efficiency of donor cells from fetuses with loss or gain of KAT6B compared with wild-type cells 18 h post-transplant (Figure S3).

Loss of KAT6B functionally impairs HSCs in transplantation assays

To assess the cell intrinsic reconstitution capacity of the HSCs, 100 CD45.2$^+$ LIN$^-$SCA1$^+$KIT$^+$CD48$^-$CD150$^+$ HSCs were sorted, combined with 2 × 10^5 whole bone marrow cells from CD45.1$^+$ or CD45.1/2$^+$ adult mice, and transplanted into lethally irradiated recipients (primary transplant; Figure 4A). Reconstitution was assessed at 4 weeks after transplantation in the peripheral blood and at 15 weeks in the peripheral blood and bone marrow. Following the primary transplant, CD45.2$^+$ LIN$^-$SCA1$^+$ KIT$^+$CD48$^-$CD150$^+$ HSCs were resorted from the bone marrow of primary recipients and transplanted into new irradiated recipients with fresh competitor adult bone marrow cells (secondary transplant; Figure 4A).

At 4 weeks post-transplant, *Kat6b*$^{-/-}$ HSC recipients showed a 61%–98% reduction in CD45.2$^+$ peripheral blood B cells and myeloid cells, but not in T cells (p = 0.02 to 0.003; Figure S4). At 15 weeks post-transplantation, a 73%–81% reduction in reconstitution with *Kat6b*$^{-/-}$ cells was observed in all peripheral blood cell types, and reconstitution by *Kat6b*$^{+/-}$ cells was also reduced (p = 0.049 to 0.02; Figure 4B). Only two of the five *Kat6b*$^{-/-}$ fetal liver donors were able to competitively reconstitute the peripheral blood of the recipients. A reduction in successful peripheral blood reconstitution was also noted in the *Kat6b*$^{+/-}$ donors, where only four of seven donors were able to contribute to the reconstituted hematopoietic system.

Kat6b$^{-/-}$ cells showed a 79%–93% reduction in reconstitution across bone marrow stem and progenitor cell populations (p = 0.003) and *Kat6b*$^{+/-}$ cells had a 52%–66% reduction in representation in the HSC and HPC-1 populations, compared with wild-type controls (p = 0.05 to 0.02; Figures 4C and 4D).

Tg(Kat6b) cell representation was increased in peripheral blood 4 weeks after transplantation (p = 0.02; Figure 4E), but no significant effect of the *Tg(Kat6b)* transgene was observed at 15 weeks post-transplant in either the blood or bone marrow (Figure S5). This suggests that overexpression of KAT6B affects only the short-term proliferation of progenitors.

Only two of the original five original *Kat6b*$^{-/-}$donors yielded enough cells for a secondary transplant of 100 HSCs. At 4 weeks after the secondary transplant, the total CD45.2$^+$ reconstitution in *Kat6b*$^{-/-}$ cell recipients was reduced to 2% compared with wild-type cell recipients (p = 0.002; Figure S4). At 15 weeks post-transplant, secondary recipients displayed 37%–90% reduced *Kat6b*$^{-/-}$ cell reconstitution in peripheral blood populations and 69%–90% reduced *Kat6b*$^{-/-}$ cell contribution to bone marrow HSC, MPP, HPC-1, HPC-2, GMP, and CLP populations (p = 0.002 to 0.0001; Figures 4F–4H). *Kat6b*$^{+/-}$ cell recipients showed a reduced percentage of CD45.2$^+$ B cells and total live cells at 15 weeks in the peripheral blood (p = 0.03 to 0.01; Figure 4F). Conversely, the *Tg(Kat6b)* transgene had no effect on the reconstitution capacity of the secondary transplants (Figure S5).

KAT6B acetylates histone H3 lysine 9 in fetal liver LSKs and HSCs

To determine the histone acetylation target of KAT6B and KAT6A in hematopoietic cell types, intranuclear immunodetection and flow cytometry was performed on E14.5 fetal liver hematopoietic cells. In parallel, western immunoblotting was performed on sorted E14.5 fetal liver LSK-derived histones.

By intranuclear flow cytometry (Figure 5A), H3K9ac levels were reduced in *Kat6b*$^{-/-}$ LSK cells relative to controls (p = 0.01; Figure 5B) and in a gene-dose-dependent manner in HSCs from *Kat6b*$^{+/-}$ and *Kat6b*$^{-/-}$ mutants to 78% (p = 0.03) and 69% (p = 0.006), respectively (Figure 5B). By western immunoblotting, H3K9ac levels were reduced in *Kat6b*$^{+/-}$ samples (p = 0.049, Figure 5C)

Figure 3. Deletion of *Kat6b* causes a reduction in multilineage contribution of fetal liver cells in competitive transplantation assays

(A) Experimental design.

(B–D) Gating strategy (B) and percentage contribution of CD45.2$^+$ donor cells from *Kat6b*$^{+/+C57BL/6}$, *Kat6b*$^{+/-}$, or *Kat6b*$^{-/-}$ donor fetuses, to peripheral white blood cells at 4 weeks (C) and 20 weeks (D) post-transplantation.

(E–G) Gating strategy (E) and percentage contribution (F and G) of CD45.2$^+$ donor cells from *Kat6b*$^{+/+C57BL/6}$, *Kat6b*$^{+/-}$, or *Kat6b*$^{-/-}$ fetal livers at 20 weeks post-transplantation. N = 4–7 fetal liver donors per genotype. Data are presented as mean ± SEM, analyzed by two-way ANOVA with Tukey (C, D, F, and G) post hoc correction. Each circle represents the average of three transplant recipient mice that received cells from a single donor. Granulo: granulocyte, Mono: monocyte, HSC: hematopoietic stem cell, MPP: multipotent progenitor cell, HPC-1: restricted hematopoietic progenitor type 1, HPC-2: restricted hematopoietic progenitor type 2, CMP: common myeloid progenitor GMP: granulocyte, macrophage progenitor, MEP: megakaryocyte, erythrocyte progenitor, CLP: common lymphoid progenitor.

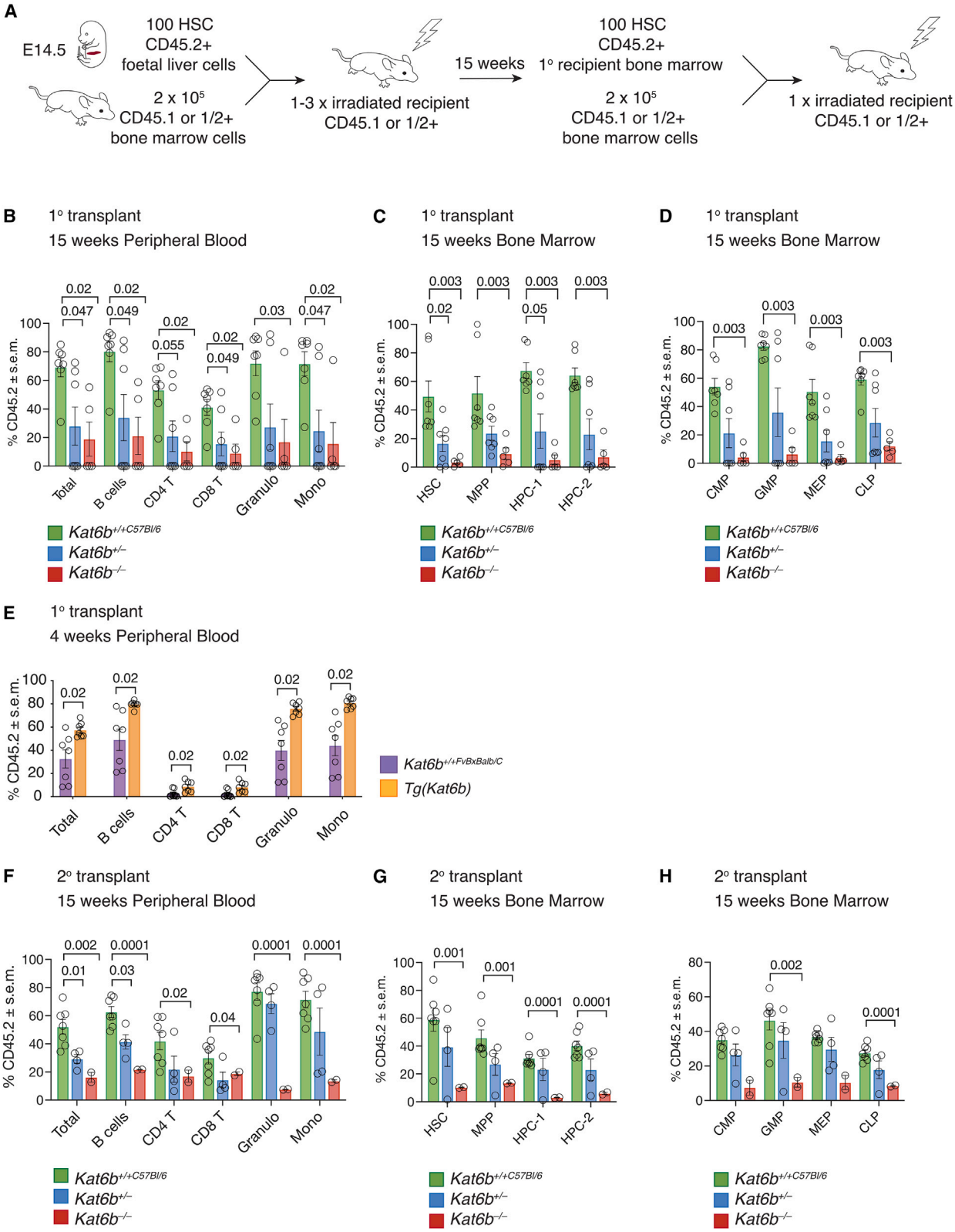

(legend on next page)

and 16% reduced in *Kat6b*$^{-/-}$ samples (p = 0.001; Figure 5C). Conversely a 45% increase in H3K9ac was observed in *Tg(Kat6b)* LSK cells (p = 0.055; Figure 5D) and HSC (p = 0.04; Figure 5D) populations by intranuclear flow cytometry and 1.2-fold increase in LSKs by western immunoblotting (p = 0.049; Figure 5E). No significant effect of KAT6B change was observed on H3K14ac or H3K23ac levels (Figure S6).

KAT6A heterozygosity caused a 29% and 33% reduction in H3K23ac in LSK (p = 0.002) and HSC (p = 0.0004) populations by intracellular flow cytometry (Figure 5F) and 15% decrease in LSKs by western immunoblotting (p = 0.008; Figure 5G). H3K9ac and H3K14ac were not significantly affected in *Kat6a*$^{+/-}$ samples (Figure S6). Last, *Kat6b*$^{+/-}$*Kat6a*$^{+/-}$ compound heterozygous samples showed a 35% and 28% reduction in H3K9ac by intracellular flow cytometry in LSK (p = 0.046) and HSC (p = 0.02) populations by intranuclear flow cytometry (Figure 5H). H3K9ac was not significantly reduced in LSKs by western immunoblotting (p = 0.06; Figure 5I). Last, H3K23ac was 33% and 43% reduced in LSK (p = 0.03) and HSC (p = 0.03) populations by intranuclear flow cytometry (Figure 5J) and 30% in LSKs by western immunoblotting (p = 0.002; Figure 5K). H3K14ac levels were comparable between compound mutant and control samples (Figure S6).

KAT6B and KAT6A promote the expression of HSC genes

To investigate potentially shared molecular functions, RNA-sequencing was performed on LSK cells sorted from *Kat6b*$^{-/-}$, *Kat6a*$^{+/-}$, *Kat6b*$^{+/-}$*Kat6a*$^{+/-}$, and wild-type E14.5 fetal livers (Figure 6A). The analysis examined annotated protein-coding genes.

Three genes were differentially expressed between *Kat6b*$^{-/-}$ and wild-type LSK cells (false discovery rate [FDR] <0.05; Figures 6B and 6C; Table S4). In contrast, 3162 genes were differentially expressed in *Kat6a*$^{+/-}$ compared with wild-type LSK cells (Tables S5). In the mutually expressed set of 7650 genes, more genes were differentially expressed in *Kat6a*$^{+/-}$ samples than in *Kat6b*$^{-/-}$ samples (2607 vs. 3; $p < 10^{-6}$, pbinom).

The expression of 4044 of 7650 expressed genes was changed in the same direction in *Kat6b*$^{-/-}$ LSK cells as in *Kat6a*$^{+/-}$ LSK cells but weaker, placing the *Kat6b*$^{-/-}$ samples between the *Kat6a*$^{+/-}$ and the wild-type samples. Robust regression analysis revealed a high correlation between gene expression changes in *Kat6b*$^{-/-}$ vs. wild-type LSK cells and in *Kat6a*$^{+/-}$ vs. wild-type LSK cells ($p < 10^{-6}$; Figure S7). Multidimensional scaling (Figure 6D) also placed *Kat6b*$^{-/-}$ samples between wild-type and *Kat6a*$^{+/-}$ samples. *Kat6b*$^{+/-}$*Kat6a*$^{+/-}$ compound heterozygous LSK cells, caused a greater disruption of gene expression than heterozygous loss of *Kat6a* alone, in a mutually expressed gene set of 8023 genes (4207 vs. 2937; $p < 10^{-6}$, pbinom; Table S6). Genes downregulated in *Kat6a*$^{+/-}$ LSK cells were enriched in gene ontology terms and Kyoto Encyclopedia of Genes and Genomes pathways that included terms relating to hematopoiesis (Table S5). These terms were even further enriched among genes downregulated in *Kat6b*$^{+/-}$*Kat6a*$^{+/-}$ compound heterozygous LSK cells (Table S6).

Thirty-eight genes were differentially expressed between *Tg(Kat6b)* and wild-type LSK cells (Table S7). This included genes encoding transcriptional regulators of hematopoiesis: *Hoxa9, Gata2, Erg,* and *Meis1* (Figures 6E and 6F).

Genes expressed in HSCs were significantly downregulated in *Kat6a*$^{+/-}$ compared with wild-type LSK cells (Figure 6G), including transcriptional regulators of hematopoiesis: *Meis1, Pbx1, Hoxa9,* and *Hoxa10* (Figure 6H). Genes differentially expressed in *Kat6a*$^{+/-}$ LSK cells negatively correlated with those dysregulated in *Meis1/Hoxa9* overexpressing relative to healthy bone marrow HSCs (Wang et al., 2010) (Figure 6I). *Kat6b*$^{+/-}$*Kat6a*$^{+/-}$ compound heterozygous LSK cells showed pronounced downregulation of genes expressed in HSCs (Figure 6J), downregulation of the transcriptional regulators of hematopoiesis affected in *Kat6a*$^{+/-}$ samples and, moreover, downregulation of additional HSC regulatory genes, including *Flt3, Erg, Gata2, Gata3,* and additional *Hoxa* genes (Figure 6K vs. 6H). A significant negative correlation was also observed between genes differentially expressed between *Kat6b*$^{+/-}$*Kat6a*$^{+/-}$ LSK cells and controls and those genes affected in leukemia cells overexpressing *Meis1/Hoxa9*

Figure 4. Sorted *Kat6b*$^{+/-}$ and *Kat6b*$^{-/-}$ HSCs show impaired short and long-term multilineage reconstitution

(A) Experimental design.

(B–D) Percentage contribution of CD45.2^{+} *Kat6b*$^{+/+C57BL/6}$, *Kat6b*$^{+/-}$, or *Kat6b*$^{-/-}$ fetal liver donor cells to peripheral white blood cells (B) and bone marrow cells (C and D) at 15 weeks post-transplantation.

(E) Percentage contribution of CD45.2^{+} *Kat6b*$^{+/+FVBxBALB/c}$ and *Tg(Kat6b)* cells to peripheral white blood cells at 4 weeks post-transplantation.

(F–H) Percentage contribution of CD45.2^{+} *Kat6b*$^{+/+C57BL/6}$, *Kat6b*$^{+/-}$, or *Kat6b*$^{-/-}$ cells from primary recipients to peripheral white blood cells (F) and bone marrow cells (G, H) in the secondary recipient mice at 15 weeks post-transplantation. N = 4–7 mice per genotype in primary transplants; N = 2–7 primary recipients per genotype in secondary transplants. Data are presented as mean ± SEM and analyzed using Mann-Whitney (B, C, D, F, G, and H) or Welch t tests (E). Each circle represents the average of transplant recipients that received cells from a single fetal liver donor (B–E) or a single secondary transplant recipient (F and G). Abbreviation as in Figure 3.

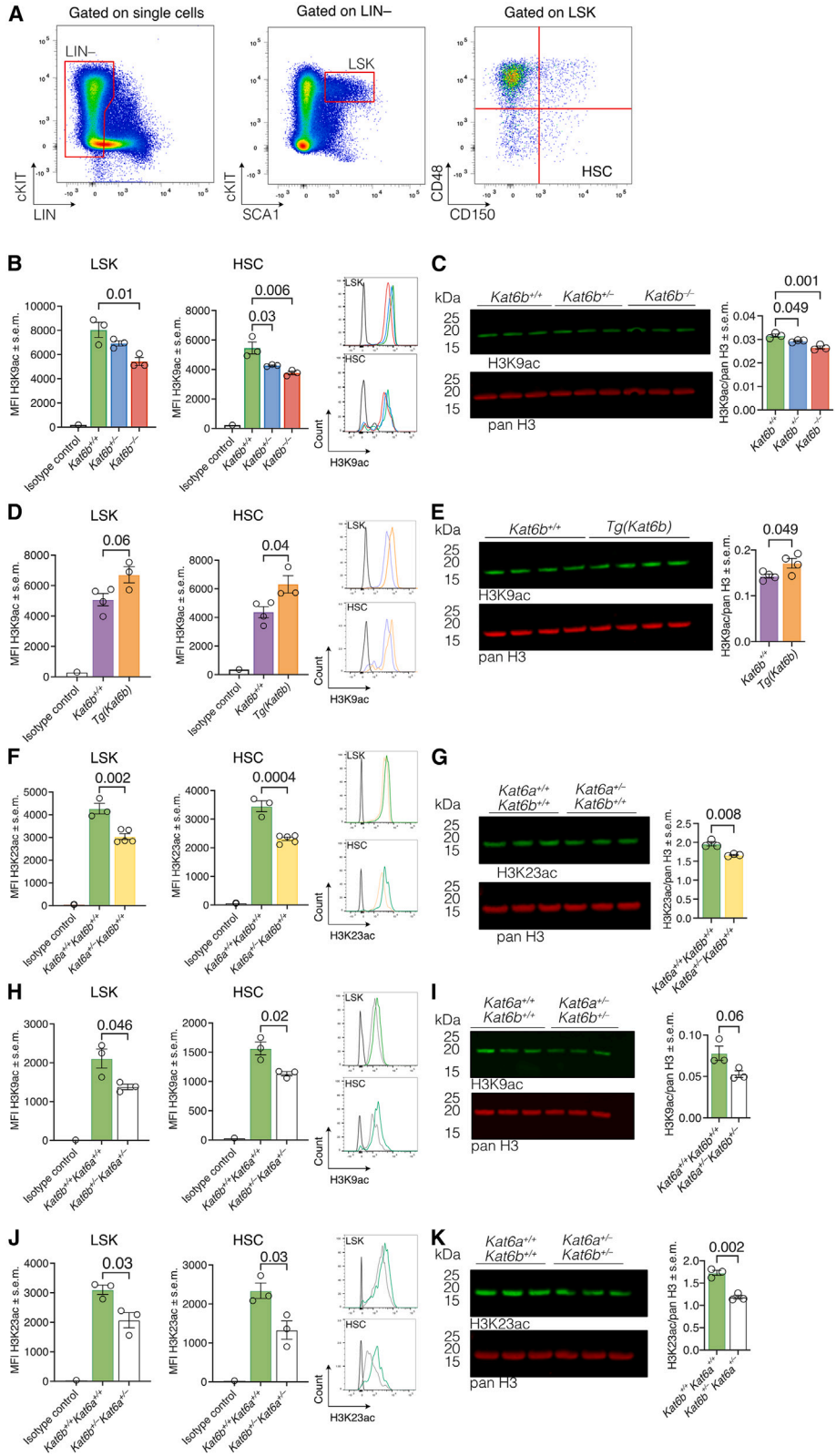

(legend on next page)

(Figure 6L). Together, this analysis suggests that, although less potent, KAT6B regulates a similar network of genes as KAT6A.

KAT6A and KAT6B exist as mutually exclusive catalytic subunits of a shared multiprotein complex, which includes BRPF1 (Doyon et al., 2006). BRPF1 can also form a complex with KAT7 (Doyon et al., 2006). We correlated genes differentially expressed in *Kat6a*$^{+/-}$*Kat6b*$^{+/-}$ LSK cells compared with controls, with those affected by BRPF1 (You et al., 2016) or KAT7 (*Kat7*$^{fl/flCre}$) deficiency (Yang et al., 2022). We found a positive correlation between differentially expressed genes in *Brpf1*^{vKO} LSK cells and those in *Kat6a*$^{+/-}$*Kat6b*$^{+/-}$ LSK cells (Figure S7; $R^2 = 0.13$) and *Kat7*$^{fl/fl\ Cre}$ LSK cells (Figure S7; $R^2 = 0.10$). Unexpectedly, we found a strong correlation between *Kat6a*$^{+/-}$*Kat6b*$^{+/-}$ and *Kat7*$^{fl/fl\ Cre}$ LSK cells (Figure S7; $R^2 = 0.40$), suggesting that these MYST family members co-regulate the expression of many genes. A total of 569 genes were downregulated in all mutants, including *Kit, Hoxa, Mecom, Mpl, Erg, Pbx1,* and *Runx1* (Figure S7). Genes commonly downregulated in BRPF1 and KAT7-deficient cells only included genes regulating erythropoiesis, *Gata1, Lmo2, Tal1, Gfib, Klf1, Sox6, Brgm, Alad, Abcg2,* and *Slc11a2* (Figure S7). Genes commonly downregulated in BRPF1 and KAT6A/KAT6B-deficient LSK cells included key marker genes and gene regulating B cell development, such as *Blnk, Bank1, CD19, Prckb,* and *Snx2* (Figure S7). Genes commonly downregulated in *Kat6b*$^{+/-}$*Kat6a*$^{+/-}$ and *Kat7*$^{fl/flCre}$ LSKs, but not *Brpf1*-deficient cells included regulators of DNA damage, splicing, and transcription, *Hdac7, Hdac10, Phf2, Phf20, Mecp2, Ddx17, Tcf20, Zeb2, Mlxip,* and *Foxo3* (Figure S7).

Given the requirement for KAT6B in global H3K9ac in LSKs (Figures 5B and 5C) and positive association between H3K9ac at promoter regions and active transcription (Wang et al., 2008), we assessed H3K9ac levels in sorted LSK cells by chromatin immunoprecipitation (ChIP)-qPCR at the promoters of genes found to be differentially expressed by RNA-sequencint (RNA-seq). H3K9ac levels were reduced in *Kat6b*$^{-/-}$ samples at the *Igfbp5* ($p = 0.056$) and *Ccnd2* promoters but did not reach significance after Benjamini-Hochberg correction for multiple testing (Figure 6M). H3K9ac levels were 1.8- to 2.5-fold increased at the promoters of genes upregulated in *Tg(Kat6b)* vs. wild-type LSKs ($p = 0.04$ to 0.03; Figure 6N). Similarly, H3K9ac levels were reduced in genes downregulated in *Kat6a*$^{+/-}$ vs. wild-type samples ($p = 0.045$ to 0.007; Figure 6O) and in *Kat6b*$^{+/-}$*Kat6a*$^{+/-}$ vs. wild-type samples ($p = 0.04$ to 0 006; Figure 6P). These data suggest that differences in H3K9ac can partially account for gene expression differences in LSKs seen by RNA-seq.

Combined *Kat6b* and *Kat6a* heterozygosity severely impairs HSC reconstitution in irradiated recipients

Kat6a heterozygous (*Kat6a*$^{+/-}$) fetal livers showed a reduced proportion of HSCs relative to wild-type controls at E14.5 (Figure 7A) as did *Kat6b*$^{+/-}$ livers (Figures 1E and 7A). *Kat6b*$^{+/-}$*Kat6a*$^{+/-}$ double heterozygous livers showed a significantly smaller proportion of HSCs relative to wild-type and *Kat6b*$^{+/-}$ ($p = 0.02$ to $<10^{-6}$; Figures 7A and 7B).

To functionally assess these cells, sorted HSCs from wild-type, single heterozygous, and double heterozygous E14.5 fetal livers were used in a competitive transplant against adult bone marrow (Figure 7C). Fifty HSCs were used owing to the limited cell numbers available in compound heterozygous mutant livers.

Recipients of *Kat6b*$^{+/-}$*Kat6a*$^{+/-}$ cells showed minimal contribution at 4 weeks post-transplantation (Figure S7) and no contribution of CD45.2^{+} cells to peripheral blood and bone marrow stem and progenitor cell populations at 15 weeks after transplantation ($p = 0.04$ to 0.008; Figures 7D–7F). This demonstrates that combined *Kat6b*$^{+/-}$ and *Kat6a*$^{+/-}$ heterozygosity effectively eliminates the capacity of fetal liver HSCs to reconstitute the hematopoietic system of a recipient. Since recipients of *Kat6b*$^{+/-}$*Kat6a*$^{+/-}$ HSCs showed no CD45.2^{+} cell contribution in the primary transplant, it was not possible to recover sufficient cells for a secondary transplant.

Figure 5. Deletion of *Kat6b* alleles has a gene-dose-dependent effect on histone H3 lysine 9 acetylation

(A) Gating strategy.

(B and C) Median fluorescence intensity (MFI) of H3K9ac levels in *Kat6b*$^{-/-}$, *Kat6b*$^{+/-}$, and *Kat6b*$^{+/+\ C57BL/6}$ LSK cells and HSCs by intracellular flow cytometry. (C) Western immunoblot of H3K9ac and pan H3 in histones derived from *Kat6b*$^{-/-}$, *Kat6b*$^{+/-}$, and *Kat6b*$^{+/+\ C57BL/6}$ E14.5 fetal liver LSK cells. Quantitation shown beside the immunoblot.

(D) MFI of H3K9ac levels in *Kat6b*$^{+/+FVBxBALB/c}$ and *Tg(Kat6b)* E14.5 fetal liver LSK cells and HSCs by intracellular flow cytometry.

(E) Western immunoblot of H3K9ac relative to pan H3 in histones from *Kat6b*$^{+/+FVBxBALB/c}$ and *Tg(Kat6b)* fetal liver LSK cells.

(F) MFI of H3K23ac levels in *Kat6a*$^{+/-}$ and *Kat6a*$^{+/+\ C57BL/6}$ E14.5 fetal liver LSK cells and HSCs.

(G) Western immunoblot of H3K23ac relative to pan H3 in histones from *Kat6a*$^{-/-}$and *Kat6a*$^{+/+\ C57BL/6}$ fetal liver LSK cells.

(H–K) MFI of H3K9ac (H) and H3K23ac (J) levels in *Kat6b*$^{+/-}$*Kat6a*$^{+/-}$ and wild-type LSK cells and HSCs by intracellular flow cytometry (H and J) and LSK cells by western immunoblotting (I and K). N = 3–8 mice per genotype. Western blots: each lane represents histones from sorted LSKs of one fetal liver. Each circle in (C, E, G, I, and K) represents one lane. Data in all graphs are displayed as mean ± SEM, analyzed by one-way ANOVA with Tukey post hoc correction (B and C) or Student's t test (D–K). MFI: median fluorescence intensity.

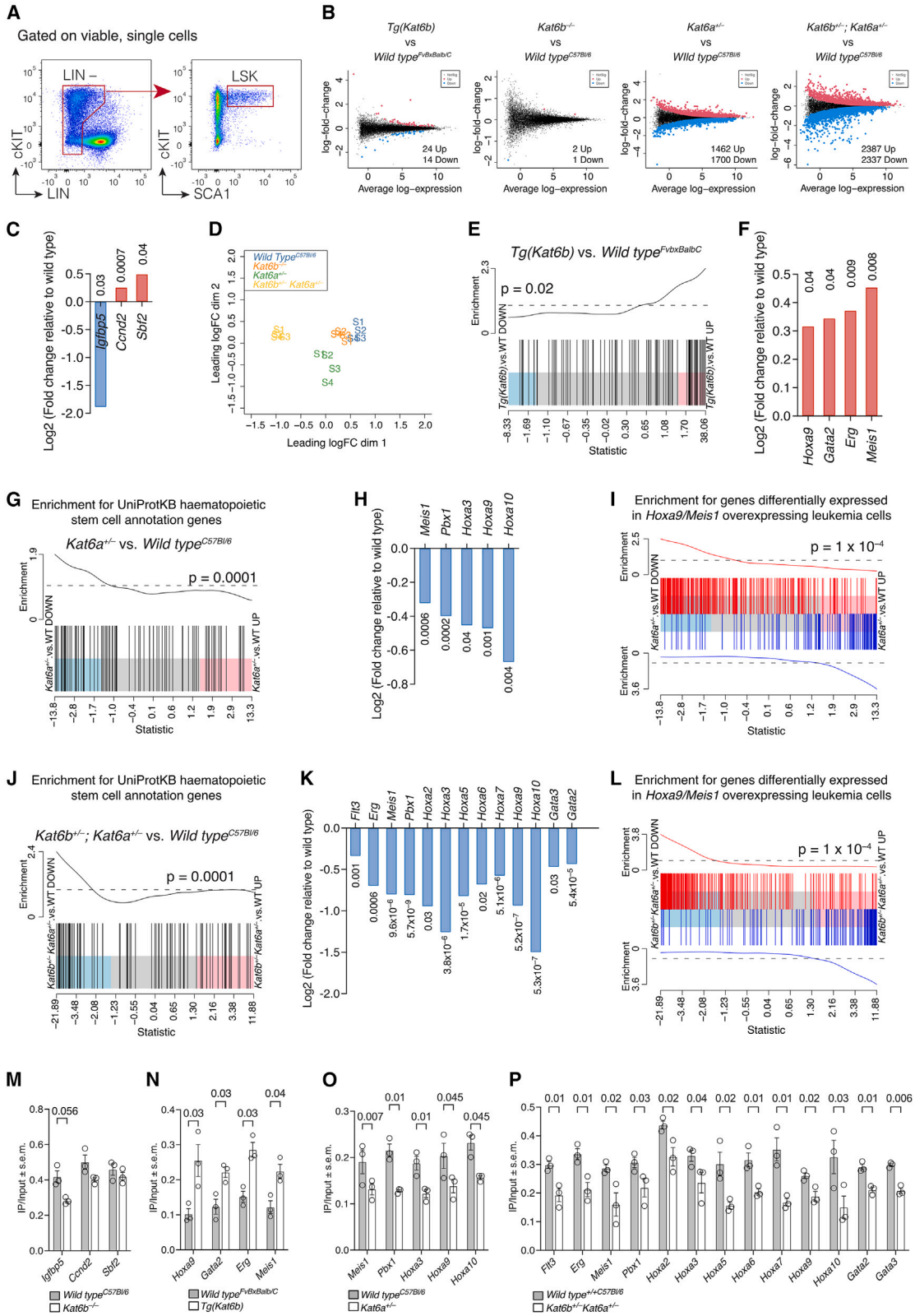

(legend on next page)

DISCUSSION

In this study, we identify the roles of KAT6B in fetal hematopoiesis and HSC function. We demonstrated that *Kat6b* gene deletion resulted in a cell intrinsic gene-dose-dependent multilineage hematopoiesis defect, including impaired multilineage hematopoietic reconstitution of lethally irradiated transplant recipients. Additionally, we showed that combined heterozygosity at both *Kat6b* and *Kat6a* genes significantly reduced HSC numbers and ablated their reconstitution capacity, suggesting that all four "KAT6" alleles were required for normal HSC development and function.

Similar to loss of one allele of *Kat6a* (Sheikh et al., 2017), loss of both alleles of *Kat6b* caused a reduction in the quiescent HSC pool and an increase in the G1 phase of the cell cycle, suggesting that KAT6A and KAT6B cooperate to maintain the quiescent HSC pool. Congruent with this interpretation, combined loss of one allele each of *Kat6a* and *Kat6a* caused a reduction in the expression of genes required to maintain the quiescent HSC pool, including *Pbx1* (Ficara et al., 2008), *Tie2* (Arai et al., 2004), and *Mpl* (Qian et al., 2007), as well as in genes required for HSC self-renewal, including *Hoxa9* (Lawrence et al., 2005), *Meis1* (Kocabas et al., 2012; Unnisa et al., 2012), and *Erg* (Ng et al., 2011).

Consistent with the role of KAT6B in leukemia (Panagopoulos et al., 2001; Vizmanos et al., 2003), *Kat6b* overexpression was found to drive expression of several factors frequently associated with hematological malignancy, including *Hoxa9* (Andreeff et al., 2008), *Meis1* (Imamura et al., 2002), and *Flt3* (Carow et al., 1996). *Tg(Kat6b)* LSK cells also showed upregulation of genes required for HSC quiescence and self-renewal.

While loss of KAT6B alone had a relatively minor effect on gene expression, we observed a strong synergistic effect when heterozygous loss of KAT6A was combined with heterozygous loss of KAT6B. Combined heterozygosity at *Kat6b* and *Kat6a* loci resulted in substantial disruptions to hematopoietic gene expression and ablated the reconstitution capabilities of HSCs. These results are of interest when considering that KAT6 inhibitors target both proteins (Baell et al., 2018; Sharma et al., 2023) and suggest that targeting KAT6B in addition to KAT6A would be of significant therapeutic benefit in hematological malignancy.

While similar to the role of KAT6A in HSC development (Thomas et al., 2006), our findings on KAT6B are somewhat discordant with a previously identified role for KAT6B in adult HSCs; short hairpin RNA (shRNA) knockdown of *Kat6b* in bone marrow HSCs from adult mice resulted in myeloid differentiation bias (Khokhar et al., 2020). Conversely, our data showed KAT6B loss in fetal HSCs

Figure 6. Loss and gain of KAT6B affect the expression of HSC genes

(A) Representative FACS plot of the LSK cell population used in RNA-seq (N = 4 fetuses per genotype). Annotated protein-coding genes were examined.

(B) Mean-difference plots comparing *Tg(Kat6b)* with $Kat6b^{+/+FVBxBALB/c}$ and $Kat6b^{-/-}$, $Kat6a^{+/-}$, and $Kat6a^{+/-}Kat6b^{+/-}$ double heterozygotes to $Kat6b^{+/+C57BL/6}$ LSK cells. Significantly downregulated genes are depicted in blue and significantly upregulated genes depicted in red.

(C) Genes differentially expressed in $Kat6b^{-/-}$ LSK cells relative to controls.

(D) Multidimensional scaling plot showing distances between transcriptional profiles. Distances on the plot represent "leading log2 fold-change" between each pair of samples.

(E) Barcode enrichment plot showing correlation between HSC-associated genes based on UniProtKB annotation: "hematopoietic stem cells" and gene expression changes in *Tg(Kat6b)* LSK cells vs. $Kat6b^{+/+FVBxBALB/c}$ controls. Vertical lines represent "hematopoietic stem cell" genes. Red and blue shaded areas are differentially expressed genesin the *Tg(Kat6b)* vs. $Kat6b^{+/+}$ LSK cells.

(F) Expression changes of specific hematopoietic regulators in *Tg(Kat6b)* LSK cells vs. wild-type.

(G) Barcode enrichment plot showing correlation between HSC-associated genes and gene expression changes in $Kat6a^{+/-}$ LSK cells vs. wild-type cells.

(H) Expression changes of specific hematopoietic regulators in $Kat6a^{+/-}$ LSK cells vs. wild-type cells.

(I) Barcode enrichment plot showing an inverse correlation between genes differentially expressed in leukemia cells compared with HSCs from dataset GSE20377 (Wang et al., 2010) and genes differentially expressed in $Kat6a^{+/-}$ LSK cells vs. wild-type cells.

(J) Barcode enrichment plot showing correlation between HSC-associated genes and gene expression changes in $Kat6b^{+/-}Kat6a^{+/-}$ LSK cells vs. wild-type controls.

(K) Expression changes of specific hematopoietic regulators in $Kat6b^{+/-}Kat6a^{+/-}$ LSK cells vs. wild-type cells.

(L) Barcode enrichment plot showing an inverse correlation between genes differentially expressed in leukemia compared with HSCs from dataset GSE20377 (Wang et al., 2010) and genes differentially expressed in $Kat6b^{+/-}Kat6a^{+/-}$ LSK cells vs. wild-type cells.

(M–P) Chromatin immunoprecipitation (ChIP) qPCR IP/Input assessment of H3K9ac levels at the promoter region of genes differentially expressed in $Kat6b^{-/-}$ (M), *Tg(Kat6b)* (N), $Kat6a^{+/-}$ (O) and $Kat6b^{+/-}Kat6a^{+/-}$ (P) LSKs vs. genetic background-matched controls. Data were analyzed as described under RNA-sequencing analysis in the methods section (A–L). Data in (M)–(P) presented as mean ± SEM and analyzed using multiple t tests with Benjamini-Hochberg corrections for multiple testing. Each circle in (M)–(P) represents IP/Input of LSKs derived from an individual fetal liver per genotype.

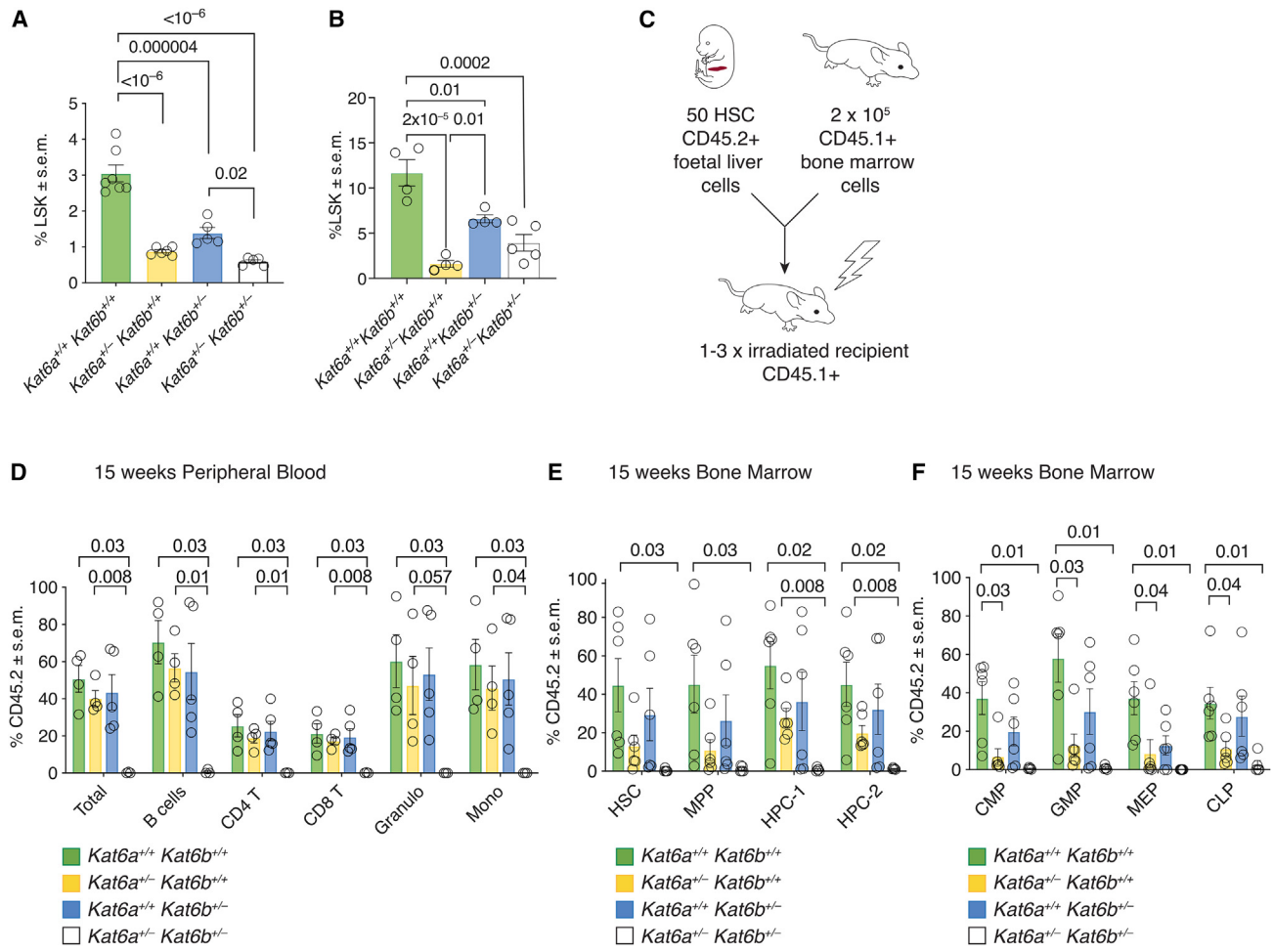

Figure 7. Combined heterozygosity at *Kat6b* and *Kat6a* results in the absence of long-term repopulating HSCs in the fetal liver

(A and B) Percentage HSCs within the LSK population of E14.5 fetal livers (A) and adult bone marrow (B) from wild-type, *Kat6a*$^{+/-}$ heterozygous, *Kat6b*$^{+/-}$ heterozygous, and *Kat6a*$^{+/-}$*Kat6b*$^{+/-}$ compound heterozygous animals.

(C) Experimental design.

(D and E) Percentage contribution of CD45.2^{+} donor cells at 15 weeks post-transplantation in the peripheral blood (D) and bone marrow (E and F). Bone marrow populations were separated by CD48 vs. CD150 (E) and CD34/CD16/CD32 or IL7R ∝ staining (F). N = 5–7 (A), 4–5 (B), and 3–5 fetal liver donor mice (D–F) per genotype. Data are presented as mean ± SEM and were analyzed using a one-way ANOVA with Tukey post hoc correction (A and B) or Welch t tests (D–G). Each circle represents a single fetal liver (A), bone marrow from a single adult animal (B), or the average of transplant recipients that received cells from a single fetal liver donor (D–F). Abbreviation as in Figure 3.

impaired reconstitution across all cell types, indicating a stem cell defect. This difference may reflect different requirements for KAT6B in the developing vs. adult hematopoietic systems. In addition, the viral transduction and 48-h culture of adult sorted HSCs required for shRNA knockdown may have allowed cells to differentiate toward a biased progenitor state and affect later behaviors, as acknowledged by the authors (Khokhar et al., 2020).

We observed reduced acetylation at H3K9, but not H3K14 or H3K23, in *Kat6b*$^{-/-}$ fetal liver HSCs. Congruently, we found that overexpression of KAT6B resulted in an increase in H3K9ac. In other studies, KAT6B has been shown to acetylate H3K23 in small cell lung cancer cells (Simo-Riudalbas et al., 2015) and K562 and 293T cell lines (Klein et al., 2019), with no effect on H3K9ac or H3K14ac described. KAT7, by comparison, is required for global H3K14ac levels in a variety of cell types (Kueh et al., 2011, 2023), while KAT6A has been shown to be required for H3K9ac *in vivo* at specific loci (Voss et al., 2009, 2012) and H3K23 in glioblastoma cell lines *in vitro* (Lv et al., 2017). Consistently, we observed a global reduction in H3K23ac in *Kat6a*$^{+/-}$ fetal liver cells and reduction in both H3K9ac and H3K23ac when both KAT6B and KAT6A were deficient. Interestingly, dual inhibitors of

both KAT6A and KAT6B reduces H3K23ac in breast cancer cells to low levels (Sharma et al., 2023). Together these results suggest that the histone target of these nuclear enzymes is tightly regulated and context dependent and that KAT6B predominantly acetylates H3K9, while H3K23 is the primary lysine acetylation target of KAT6A in hematopoietic cells.

In addition, we combined our RNA-seq LSK datasets with publicly available data assessing deficiency in BRPF1 (You et al., 2016), a chromatin binding protein found in the KAT6A/B and KAT7 multiprotein complexes (Doyon et al., 2006). Like KAT6A (Thomas et al., 2006) and KAT6B, KAT7 also has a critical role in maintaining HSC function (Yang et al., 2022). We found that genes commonly downregulated in all three mutants were enriched for HSC quiescence and self-renewal genes. This is consistent with impaired HSC numbers and reconstitution described in BRPF1 (You et al., 2016), KAT7 (Yang et al., 2022), KAT6A (Thomas et al., 2006), and KAT6B single mutants and indicates that a full suite of BRPF1, KAT7, KAT6A, and KAT6B is required to maintain the HSC pool. Interestingly, the double PHD domain of KAT6B has been shown to bind histone H3 acetylated on lysine 14 (Klein et al.), consistent with the notion that KAT6A/B and KAT7 cooperate to maintain the undifferentiated HSC pool. Conversely, we found that genes downregulated in BRPF1 and KAT7 datasets, but not in KAT6A/B LSK cells, were enriched for drivers of the erythroid lineage, while those affected by BRPF1 and KAT6A/B, but not KAT7, included regulators of B cell development. This is consistent with a previously identified role for KAT7 in erythroid cell differentiation (Mishima et al., 2011) and requirement for KAT6A in B cell progenitor populations (Sheikh et al., 2015), in addition to HSCs. These observations suggest that, while the HSC population has a non-redundant requirement for BRPF1, KAT6A, KAT6B, and KAT7, it is their unique complex combinations and binding activities that confer differentiation down the erythroid or alternative lineages.

In conclusion, our findings suggest that there is a high degree of cooperation in the regulation of hematopoiesis by the MYST family chromatin regulators KAT6A and KAT6B. The results shown here have important implications for the development and use of small molecular inhibitors against KAT6A and KAT6B, suggesting there may be therapeutic benefit to simultaneously targeting both proteins in hematological malignancy, as well as informing on the potential for on-target side effects. Additionally, these findings, in combination with previously published work, indicate a mechanism for HSC lineage commitment, based on the combinatorial effects of MYST family histone lysine acetyltransferases and auxiliary complex members.

EXPERIMENTAL PROCEDURES

Resource availability

Lead contact

Requests for further information and resources should be directed to Tim Thomas.

Materials availability

Requests for reagents should be directed to Tim Thomas.

Data and code availability

High throughput sequencing data is publicly available under GEO accession number GSE256039. This paper does not report custom code.

Mice

The *Kat6b* locus was targeted twice to generate a null allele, resulting deletion of exons 2–12 of the *Kat6b* gene (Figure S1). Compound heterozygosity at *Kat6a* and *Kat6b* loci was perinatally lethal on a C57Bl/6 background. To increase the animals' vigor, $Kat6b^{+/-}$ and $Kat6a^{+/-}$ heterozygous animals were crossed to FVB:BALB/c F1 hybrid mice, which were intercrossed to yield $Kat6b^{+/-}Kat6a^{+/-}$, approximately 20% of the expected number survive until adulthood. KAT6B overexpressing mice were generated using a *pBACe3.6* clone *RP23-360F23* carrying the wild-type *Kat6b* allele, including 21 kb 5′ and 42 kb 3′ of the coding exons. All regulatory sequences necessary to recapitulate the expression pattern are included in sequences 5′ of the first coding exon 2 and gene body to exon 14 (Sheikh et al., 2012). Seven copies inserted into the genome, resulting in a 5-fold increase in *Kat6b* expression (Figure S1). At E14.5 $Kat6b^{-/-}$and *Tg(Kat6b)* fetuses were indistinguishable from wild-type littermates (Figure S1). Mice were genotyped by PCR to identify the *Kat6b* wild-type allele and null allele or *SacB* in the *BAC* vector to identify *Tg(Kat6b)* mice (Figure S1). Mouse husbandry and experiments were conducted in accordance with the Australian code for the care and use of animals for scientific purposes and with the approval of the Walter and Eliza Hall Animal Ethics Committee.

Transplantation assays

Adult bone marrow cells were combined with fetal liver cells at numbers determined using a hematology analyzer (Advia 2120i) or with 50 or 100 sorted HSC cells, isolated using an Aria W (FACS Aria II SORP) cell sorter. Cells were injected intravenously into lethally irradiated recipient mice (2 × doses 5.5 Gy, 3 h apart) as previously described (Sheikh et al., 2016).

Colony-forming assay

A total of 1×10^5 fetal liver cells, as determined using a hematology analyzer, were cultured in 0.3% agar in Dulbecco's modified Eagle's medium supplemented with purified murine growth factors; interleukin-3 (IL-3; 10^{-3} U/mL; made in house), stem cell factor (SCF; 100 ng/mL), and erythropoietin (EPO; 2 U/mL), or with saline as a negative control. Cultures were incubated for 7 days prior to fixation and staining. Colonies were counted and identified as described (Metcalf, 1984). Colonies were imaged using a compound microscope (Zeiss) and colony sizes quantified in Fiji (version 2.14.0/1.54f).

Flow cytometry for cell surface markers

Cells were analyzed on the LSR II W. Cell sorting was conducted on an Aria W cell sorter, using antibodies described in Tables S2 and S3. All collected data were subsequently analyzed using FlowJo 10.1r5.

Intranuclear flow cytometry for histone acetylation markers

Cells were fixed and permeabilized using the FOXP3 Transcription Factor Staining Buffer Set (Thermo Scientific; 00-5523-00) supplemented with sodium butyrate and EDTA-free protease inhibitors. Cytometry was performed using LSR II W (BD Biosciences) and analyzed using FlowJo 10.1r5.

Annexin V and PI staining

Cells were incubated with antibodies (Table S3) and stained using the Annexin V/Dead cell apoptosis kit for flow cytometry according to the manufacturer's instructions and analyzed on the LSR II W.

Ki67 and DAPI staining

Cells were incubated with antibodies and resuspended in 250 μL Cytofix/Cytoperm solution and analyzed on the LSR II W at less than 3000 events/s and analyzed using FlowJo 10.1r5.

RNA-sequencing of sorted LSK cells and analysis

E14.5 fetal livers were harvested and LSK cells were sorted, RNA purified, sequenced, and analyzed essentially as described previously (Yang et al., 2022). For detailed information of the procedures, see supplementary methods.

Western immunoblotting of sorted LSK cells

E14.5 fetal liver LSKs were sorted and histones extracted using TCA acid; 250 ng–2 μg isolated histones were run on NuPAGE 4–12% Bis-Tris polyacrylamide gels (ThermoFisher, NP0322) transferred onto nitrocellulose membranes (Licor, 926–31090), blocked using Intercept (PBS) Blocking buffer (Licor, 927–70001), incubated with primary antibodies against acetylated histones (Table S2), then incubated with secondary antibodies (Table S2) in Intercept (PBS) Blocking buffer. Membranes were washed again, imaged, and analyzed using LiCor software.

Chromatin immunoprecipitation qPCR of sorted LSK cells

E14.5 fetal liver LSKs were sorted, and chromatin immunoprecipitation was performed using the ChIP-IT High-Sensitivity kit. Samples were sonicated using a Covaris focused ultra-sonicator ME220 instrument under the following conditions: Duty Factor: 20; 200 cycles/burst; 75-watt peak power; 60 s duration. Immunoprecipitation was performed using an anti-acetyl-Histone H3 Lysine 9 antibody (Cell Signaling, 9649). Precipitated DNA was analyzed on a QuantStudio qPCR machine using gene-specific primers (Table S4). Primers were designed using Primer3.

Statistics

The statistical analysis methods for the RNA-seq data are provided above under RNA-seq analysis. Pbinom was calculated in R. Other data are presented as circles for individual animals with mean ± SEM. Statistical analyses for all flow cytometry data were performed in Prism GraphPad Version 8.3.1. Student's t test with correction for multiple testing was used in experiments where two genotypes were compared. ANOVA with correction for multiple testing was used in experiments where three genotypes were compared. When unequal variance was observed, multiple t tests with Welch correction and correction for multiple testing were used. When unequal variance and lack of normal distribution were observed, multiple t tests with Mann-Whitney correction and correction for multiple testing were used. Statistical tests employed and number of biological replicates are specified in the figure legends of the results section.

SUPPLEMENTAL INFORMATION

Supplemental information can be found online at https://doi.org/10.1016/j.stemcr.2024.02.005.

ACKNOWLEDGMENTS

The authors would like to thank N. Blasch and L. Johnson for expert animal care; L. Potenza and C. Burström for excellent technical assistance; and the WEHI FACS facility, especially Simon Monard and Julie Tellier.

This work was supported by the Australian NHMRC: Project Grant 1084248; Program Grant 1113577; Research Fellowships: 1155342 to S.L.N., 1058344 to W.S.A., and 1154970 to G.K.S.; Investigator Grant 1176789 to A.K.V. through the Independent Research Institutes Infrastructure Support Scheme; and by the Victorian Government through an Operational Infrastructure Support Grant. S.N.W. was supported by the Walter and Eliza Hall Trust Centenary Fellowship, an NHMRC Ideas grant 1184523 (S.L.N. and S.N.W.) and the Leukemia & Lymphoma Society-Snowdome Foundation-Leukaemia Foundation (LLS-SF-LF; 6592-20) Translational Research Program (TRP) (S.L.N. and S.N.W.).

National Health and Medical Research Council.

AUTHOR CONTRIBUTIONS

Contributions: M.I.B., S.N.W., A.D., H.M.M., Y.Y., L.D.R., and S.W. carried out experiments. N.K., W.A., C.S.N.L.-W.-S., and A.L.G. performed bioinformatics analyses supervised by G.K.S. S.L.N. and W.S.A. provided advice. M.I.B., A.K.V., and T.T. wrote the manuscript. A.K.V. and T.T. jointly conceived the study and supervised the project.

DECLARATION OF INTERESTS

T.T. and A.K.V. are inventors on patent WO2016198507 A1. The Thomas and Voss laboratories received research funding from the CRC for Cancer Therapeutics (CTx), Australia. T.T. and A.K.V. have received payments from a distribution of licensing income from Pfizer and have served on an advisory board for Pfizer.

Received: August 24, 2023
Revised: February 20, 2024
Accepted: February 20, 2024
Published: March 21, 2024

REFERENCES

Adelman, E.R., Huang, H.T., Roisman, A., Olsson, A., Colaprico, A., Qin, T., Lindsley, R.C., Bejar, R., Salomonis, N., Grimes, H.L., and Figueroa, M.E. (2019). Aging human hematopoietic stem cells manifest profound epigenetic reprogramming of enhancers that may predispose to leukemia. Cancer Discov. *9*, 1080–1101.

Andreeff, M., Ruvolo, V., Gadgil, S., Zeng, C., Coombes, K., Chen, W., Kornblau, S., Barón, A.E., and Drabkin, H.A. (2008). HOX expression patterns identify a common signature for favorable AML. Leukemia *22*, 2041–2047.

Arai, F., Hirao, A., Ohmura, M., Sato, H., Matsuoka, S., Takubo, K., Ito, K., Koh, G.Y., and Suda, T. (2004). Tie2/angiopoietin-1 signaling regulates hematopoietic stem cell quiescence in the bone marrow niche. Cell *118*, 149–161.

Baell, J.B., Leaver, D.J., Hermans, S.J., Kelly, G.L., Brennan, M.S., Downer, N.L., Nguyen, N., Wichmann, J., McRae, H.M., Yang, Y., et al. (2018). Inhibitors of histone acetyltransferases KAT6A/B induce senescence and arrest tumour growth. Nature *560*, 253–257.

Borrow, J., Stanton, V.P., Jr., Andresen, J.M., Becher, R., Behm, F.G., Chaganti, R.S., Civin, C.I., Disteche, C., Dubé, I., Frischauf, A.M., et al. (1996). The translocation t(8;16)(p11;p13) of acute myeloid leukaemia fuses a putative acetyltransferase to the CREB-binding protein. Nat. Genet. *14*, 33–41.

Campeau, P.M., Lu, J.T., Dawson, B.C., Fokkema, I.F.A.C., Robertson, S.P., Gibbs, R.A., and Lee, B.H. (2012). The KAT6B-related disorders genitopatellar syndrome and Ohdo/SBBYS syndrome have distinct clinical features reflecting distinct molecular mechanisms. Hum. Mutat. *33*, 1520–1525.

Carow, C.E., Levenstein, M., Kaufmann, S.H., Chen, J., Amin, S., Rockwell, P., Witte, L., Borowitz, M.J., Civin, C.I., and Small, D. (1996). Expression of the hematopoietic growth factor receptor FLT3 (STK-1/Flk2) in human leukemias. Blood *87*, 1089–1096.

Champagne, N., Bertos, N.R., Pelletier, N., Wang, A.H., Vezmar, M., Yang, Y., Heng, H.H., and Yang, X.J. (1999). Identification of a human histone acetyltransferase related to monocytic leukemia zinc finger protein. J. Biol. Chem. *274*, 28528–28536.

Clayton-Smith, J., O'Sullivan, J., Daly, S., Bhaskar, S., Day, R., Anderson, B., Voss, A.K., Thomas, T., Biesecker, L.G., Smith, P., et al. (2011). Whole-exome-sequencing identifies mutations in histone acetyltransferase gene KAT6B in individuals with the Say-Barber-Biesecker variant of Ohdo syndrome. Am. J. Hum. Genet. *89*, 675–681.

Doyon, Y., Cayrou, C., Ullah, M., Landry, A.J., Côté, V., Selleck, W., Lane, W.S., Tan, S., Yang, X.J., and Côté, J. (2006). ING tumor suppressor proteins are critical regulators of chromatin acetylation required for genome expression and perpetuation. Mol. Cell *21*, 51–64.

Ficara, F., Murphy, M.J., Lin, M., and Cleary, M.L. (2008). Pbx1 regulates self-renewal of long-term hematopoietic stem cells by maintaining their quiescence. Cell Stem Cell *2*, 484–496.

Imamura, T., Morimoto, A., Takanashi, M., Hibi, S., Sugimoto, T., Ishii, E., and Imashuku, S. (2002). Frequent co-expression of HoxA9 and Meis1 genes in infant acute lymphoblastic leukaemia with MLL rearrangement. Br. J. Haematol. *119*, 119–121.

Katsumoto, T., Aikawa, Y., Iwama, A., Ueda, S., Ichikawa, H., Ochiya, T., and Kitabayashi, I. (2006). MOZ is essential for maintenance of hematopoietic stem cells. Genes Dev. *20*, 1321–1330.

Khokhar, E.S., Borikar, S., Eudy, E., Stearns, T., Young, K., and Trowbridge, J.J. (2020). Aging-associated decrease in the histone acetyltransferase KAT6B is linked to altered hematopoietic stem cell differentiation. Exp. Hematol. *82*, 43–52.

Klein, B.J., Jang, S.M., Lachance, C., Mi, W., Lyu, J., Sakuraba, S., Krajewski, K., Wang, W.W., Sidoli, S., Liu, J., et al. (2019). Histone H3K23-specific acetylation by MORF is coupled to H3K14 acylation. Nat. Commun. *10*, 4724.

Kocabas, F., Zheng, J., Thet, S., Copeland, N.G., Jenkins, N.A., DeBerardinis, R.J., Zhang, C., and Sadek, H.A. (2012). Meis1 regulates the metabolic phenotype and oxidant defense of hematopoietic stem cells. Blood *120*, 4963–4972.

Kraft, M., Cirstea, I.C., Voss, A.K., Thomas, T., Goehring, I., Sheikh, B.N., Gordon, L., Scott, H., Smyth, G.K., Ahmadian, M.R., et al. (2011). Disruption of the histone acetyltransferase MYST4 leads to a Noonan syndrome-like phenotype and hyperactivated MAPK signaling in humans and mice. J. Clin. Invest. *121*, 3479–3491.

Kueh, A.J., Bergamasco, M.I., Quaglieri, A., Phipson, B., Li-Wai-Suen, C.S.N., Lönnstedt, I.M., Hu, Y., Feng, Z.P., Woodruff, C., May, R.E., et al. (2023). Stem cell plasticity, acetylation of H3K14, and de novo gene activation rely on KAT7. Cell Rep. *42*, 111980.

Kueh, A.J., Dixon, M.P., Voss, A.K., and Thomas, T. (2011). HBO1 is required for H3K14 acetylation and normal transcriptional activity during embryonic development. Mol. Cell Biol. *31*, 845–860.

Lawrence, H.J., Christensen, J., Fong, S., Hu, Y.L., Weissman, I., Sauvageau, G., Humphries, R.K., and Largman, C. (2005). Loss of expression of the Hoxa-9 homeobox gene impairs the proliferation and repopulating ability of hematopoietic stem cells. Blood *106*, 3988–3994.

Lv, D., Jia, F., Hou, Y., Sang, Y., Alvarez, A.A., Zhang, W., Gao, W.Q., Hu, B., Cheng, S.Y., Ge, J., et al. (2017). Histone acetyltransferase KAT6A upregulates PI3K/AKT signaling through TRIM24 binding. Cancer Res. *77*, 6190–6201.

Metcalf, D. (1984). The Hemopoietic Colony Stimulating Factors (Elsevier).

Mishima, Y., Miyagi, S., Saraya, A., Negishi, M., Endoh, M., Endo, T.A., Toyoda, T., Shinga, J., Katsumoto, T., Chiba, T., et al. (2011). The Hbo1-Brd1/Brpf2 complex is responsible for global acetylation of H3K14 and required for fetal liver erythropoiesis. Blood *118*, 2443–2453.

Ng, A.P., Loughran, S.J., Metcalf, D., Hyland, C.D., de Graaf, C.A., Hu, Y., Smyth, G.K., Hilton, D.J., Kile, B.T., and Alexander, W.S. (2011). Erg is required for self-renewal of hematopoietic stem cells during stress hematopoiesis in mice. Blood *118*, 2454–2461.

Panagopoulos, I., Fioretos, T., Isaksson, M., Samuelsson, U., Billström, R., Strömbeck, B., Mitelman, F., and Johansson, B. (2001). Fusion of the MORF and CBP genes in acute myeloid leukemia with the t(10;16)(q22;p13). Hum. Mol. Genet. *10*, 395–404.

Qian, H., Buza-Vidas, N., Hyland, C.D., Jensen, C.T., Antonchuk, J., Månsson, R., Thoren, L.A., Ekblom, M., Alexander, W.S., and Jacobsen, S.E.W. (2007). Critical role of thrombopoietin in maintaining

adult quiescent hematopoietic stem cells. Cell Stem Cell *1*, 671–684.

Sharma, S., Chung, C.Y., Uryu, S., Petrovic, J., Cao, J., Rickard, A., Nady, N., Greasley, S., Johnson, E., Brodsky, O., et al. (2023). Discovery of a highly potent, selective, orally bioavailable inhibitor of KAT6A/B histone acetyltransferases with efficacy against KAT6A-high ER+ breast cancer. Cell Chem. Biol. *30*, 1191–1210.e20.

Sheikh, B.N., Dixon, M.P., Thomas, T., and Voss, A.K. (2012). Querkopf is a key marker of self-renewal and multipotency of adult neural stem cells. J. Cell Sci. *125*, 295–309.

Sheikh, B.N., Lee, S.C.W., El-Saafin, F., Vanyai, H.K., Hu, Y., Pang, S.H.M., Grabow, S., Strasser, A., Nutt, S.L., Alexander, W.S., et al. (2015). MOZ regulates B-cell progenitors and, consequently, Moz haploinsufficiency dramatically retards MYC-induced lymphoma development. Blood *125*, 1910–1921.

Sheikh, B.N., Metcalf, D., Voss, A.K., and Thomas, T. (2017). MOZ and BMI1 act synergistically to maintain hematopoietic stem cells. Exp. Hematol. *47*, 83–97.e8.

Sheikh, B.N., Yang, Y., Schreuder, J., Nilsson, S.K., Bilardi, R., Carotta, S., McRae, H.M., Metcalf, D., Voss, A.K., and Thomas, T. (2016). MOZ (KAT6A) is essential for the maintenance of classically defined adult hematopoietic stem cells. Blood *128*, 2307–2318.

Simó-Riudalbas, L., Pérez-Salvia, M., Setien, F., Villanueva, A., Moutinho, C., Martínez-Cardús, A., Moran, S., Berdasco, M., Gomez, A., Vidal, E., et al. (2015). KAT6B Is a tumor suppressor Histone H3 Lysine 23 acetyltransferase undergoing genomic loss in small cell lung cancer. Cancer Res. *75*, 3936–3945.

Simpson, M.A., Deshpande, C., Dafou, D., Vissers, L.E.L.M., Woollard, W.J., Holder, S.E., Gillessen-Kaesbach, G., Derks, R., White, S.M., Cohen-Snuijf, R., et al. (2012). De novo mutations of the gene encoding the histone acetyltransferase KAT6B cause Genitopatellar syndrome. Am. J. Hum. Genet. *90*, 290–294.

Thomas, T., Corcoran, L.M., Gugasyan, R., Dixon, M.P., Brodnicki, T., Nutt, S.L., Metcalf, D., and Voss, A.K. (2006). Monocytic leukemia zinc finger protein is essential for the development of long-term reconstituting hematopoietic stem cells. Genes Dev. *20*, 1175–1186.

Thomas, T., Voss, A.K., Chowdhury, K., and Gruss, P. (2000). Querkopf, a MYST family histone acetyltransferase, is required for normal cerebral cortex development. Development *127*, 2537–2548.

Unnisa, Z., Clark, J.P., Roychoudhury, J., Thomas, E., Tessarollo, L., Copeland, N.G., Jenkins, N.A., Grimes, H.L., and Kumar, A.R. (2012). Meis1 preserves hematopoietic stem cells in mice by limiting oxidative stress. Blood *120*, 4973–4981.

Vizmanos, J.L., Larráyoz, M.J., Lahortiga, I., Floristán, F., Alvarez, C., Odero, M.D., Novo, F.J., and Calasanz, M.J. (2003). t(10;16)(q22;p13) MORF-CREBBP fusion is a recurrent event in acute myeloid leukemia. Genes Chromosomes Cancer *36*, 402–405.

Voss, A.K., Collin, C., Dixon, M.P., and Thomas, T. (2009). Moz and retinoic acid coordinately regulate H3K9 acetylation, Hox gene expression, and segment identity. Dev. Cell *17*, 674–686.

Voss, A.K., Vanyai, H.K., Collin, C., Dixon, M.P., McLennan, T.J., Sheikh, B.N., Scambler, P., and Thomas, T. (2012). MOZ regulates the Tbx1 locus, and Moz mutation partially phenocopies DiGeorge syndrome. Dev. Cell *23*, 652–663.

Wang, Y., Krivtsov, A.V., Sinha, A.U., North, T.E., Goessling, W., Feng, Z., Zon, L.I., and Armstrong, S.A. (2010). The Wnt/beta-catenin pathway is required for the development of leukemia stem cells in AML. Science *327*, 1650–1653.

Wang, Z., Zang, C., Rosenfeld, J.A., Schones, D.E., Barski, A., Cuddapah, S., Cui, K., Roh, T.Y., Peng, W., Zhang, M.Q., and Zhao, K. (2008). Combinatorial patterns of histone acetylations and methylations in the human genome. Nat. Genet. *40*, 897–903.

Yang, Y., Kueh, A.J., Grant, Z.L., Abeysekera, W., Garnham, A.L., Wilcox, S., Hyland, C.D., Di Rago, L., Metcalf, D., Alexander, W.S., et al. (2022). The histone lysine acetyltransferase HBO1 (KAT7) regulates hematopoietic stem cell quiescence and self-renewal. Blood *139*, 845–858.

You, L., Li, L., Zou, J., Yan, K., Belle, J., Nijnik, A., Wang, E., and Yang, X.J. (2016). BRPF1 is essential for development of fetal hematopoietic stem cells. J. Clin. Invest. *126*, 3247–3262.